Wasit Journal of Engineering Sciences
Journal homepage: https://ejuow.uowasit.edu.iq
ISSN 2305-6932
Original Research
Vol. 14 No. 2 June 2026, pp.101-111
https://doi.org/10.31185/ejuow.v14i2.783

An Urban Influence Radius Framework for Environmental-Spatial Evaluation in Medium-Sized Cities

Haider Majid Hasan[1], Husam Sachet Saneh [1], Ayam Sh. Altameemi [1], Noor Dheyaa Joodi[1]
[1] Architectural Engineering Department, College of Engineering, Wasit University, Wasit, Iraq.

Corresponding Author Email: hsachit@uowasit.edu.iq

Received Aug.16, 2025 | Revised Nov.6, 2025 | Accepted. Nov.19, 2025 | Online Jun.1, 2026

ABSTRACT

Medium-sized cities are densifying in ways that concentrate high-occupancy projects inside compact cores. Conventional plot-based controls such as floor area ratio, setbacks, and coverage regulate quantity rather than spatial distribution, and therefore cannot reveal off-site environmental and pedestrian effects. This paper formalizes an Urban Influence Radius and applies it to a dense hospital site in central Kut, Iraq. The Urban Influence Radius is the minimum radius R inside which a project's massing measurably alters shading, airflow, thermal comfort, and pedestrian performance. We adopt a practical baseline R = max(2H, 1.5W, 60 m), rounded to the nearest 5 m, where H is the main building height and W is the adjacent street width. Using Rhino, Grasshopper, and Ladybug Tools, we compute key performance indicators on-site and within the Urban Influence Radius. Holding FAR near 5.0, the baseline high-coverage massing performs poorly within the radius, while a lower-coverage alternative improves summer UTCI, winter solar access, wind renewal, and walkability without reducing program area. A sensitivity analysis over R = 40-80 m and coverage = 50-80 percent confirms robustness. The results support adding Urban Influence Radius screening and threshold-driven iteration to approvals and motivate an Enhanced Environmental FAR that reports FAR together with KPI compliance. The workflow is replicable with standard tools and SI units.
This research develops the Urban Influence Radius (UIR) as a quantitative framework to measure how building massing influences environmental and pedestrian conditions beyond the project boundary, addressing the shortcomings of existing density-based urban metrics in medium-sized cities.

Keywords: Urban Influence Radius, Floor Area Ratio, Grasshopper, Ladybug Tools, urban microclimate.

1. Introduction

Medium-sized cities frequently insert large institutional or commercial facilities inside mixed fabrics. Medium-Medium-sized cities, typically hosting between 300,000 and 1,000,000 inhabitants, exhibit mixed land-use and transitional densities. Kut, with about 450,000 residents and a compact core, represents this category and serves as a suitable case for applying the Urban Influence Radius (UIR) framework to evaluate urban densification impacts. Plot-based metrics such as FAR (Floor Area Ratio to defined as the ratio of the total built floor area of all stories to the plot area. For example, if a plot has an area of 1,000 m² and a building has five floors of 600 m² each, the FAR equals (5×600)/1,000 = 3.0. Higher FAR values indicate greater density regardless of building shape. FAR differs from the Coverage Ratio, which measures only the footprint area of the building divided by the plot area, without accounting for total floor area. For instance, a tall narrow tower and a low wide building could have the same Coverage Ratio but very different FAR values.) constrain total floor area but do not capture how volume is distributed and how that distribution affects the surrounding microclimate and pedestrian conditions outside the plot boundary. Recent urban climate research links sky-view factor, aspect ratios, and porosity to outdoor thermal stress and ventilation, while daylight and sunlight guidance emphasizes winter solar access on opposing façades. This paper advances a replicable framework that complements plot checks with an Urban Influence Radius analysis so that off-site effects are measured in parallel with on-site performance. This study responds to the absence of tools that link built form geometry with its off-site environmental effects. It introduces the Urban Influence Radius (UIR) as a framework for quantifying how building massing influences shading, airflow, and pedestrian comfort in medium-sized cities. The UIR describes the spatial area where built form has a very significant role to play in microclimate and walkability, hence better integrated urban planning decisions.

2. Literature Review

Urban form and microclimate analyses reveal that canyon geometry, sky-view factor, and permeability control the heat exchange, wind renewal, and solar access. Comfort indices like that of UTCI provide operational categories through which levels of interpretation of outdoor thermal stress are communicated. Pedestrian wind guidance by Lawson-type criteria has been normalized for use in transport and development projects to pick out problematic accelerations and stagnation thereby making these insights available for regulatory review via a proposed radius-based approach.

2.1. Height–Width Ratio and Thermal Comfort

Numerical microclimate modeling with ENVI-met and other models has affirmed that building height and street width control solar access, shading duration, and wind penetration. Findings by Ali-Toudert and Mayer (2006) in hot-dry climate indicated that increasing the height-to-width ratio reduced pedestrian heat stress through better shading condition, though ventilation could be reduced [1].

2.2. Density and Ventilation Performance

Computational Fluid Dynamics (CFD) simulations in actual compact urban environments-within the Tuscolano-Don Bosco district of Rome, were used-show that increasing building density reduces mean wind velocity at the pedestrian level by up to 62%. It emphasizes the importance of spatial separation and orientation to allow for adequate air circulation [2].

2.3. Ventilation Corridors and Heat Mitigation

Urban ventilation corridors are conceived as a key planning strategy in the mitigation of UHI and improvement of outdoor comfort within the compact city. High-resolution Digital Surface Models (DSM) together with wind data provided by Zhang et al. (2025) illustrate that strategically aligned open spaces and riverfront setbacks maintain the flow of air even through densely built districts [3], [4], [5].

2.4. Local Context: Al-Kut, Iraq

Al-Kut is the capital of Wasit Province. It sits on the Tigris River. There is a historic urban core, which keeps its traditional boundaries even with growth in other parts of the city. Its morphology very closely matches those parameters described by the UIR model. Tall buildings alongside narrow streets create extended shade within the area, thus providing thermal comfort in hot seasons [6], [7]. With such dense construction, natural wind penetration is minimized; hence, deliberate ventilation channels are necessary [8], [9], [10]. The Tigris offers cooling benefits and a unique riverfront microclimate, though urban pressures have limited its full utilization [11], [12], [13]. Figure 1. locates Al-Kut within Iraq and summarizes the Phase 6 Final Master Plan together with staged urban growth from 1922 to 2025, highlighting current land-use structure and the expansion of the historic core.

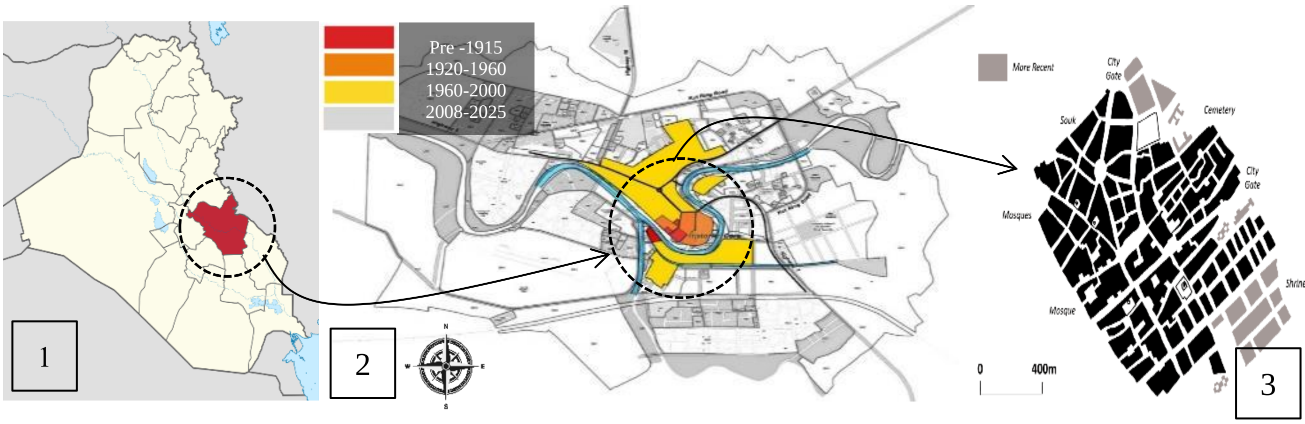

Figure 1. Kut City Master Plan – Phase 6 Final Master Plan and Historical Urban Development (1922–2025)

The Kut City Master Plan – Phase 6 Final Master Plan, issued by the Ministry of Municipalities and Public Works / General Directorate of Physical Planning – Directorate of Physical Planning in Wasit, represents the final zoning and land-use framework for the city of Kut. The plan aims to regulate and guide the city's urban growth through clearly defined land-use categories, including residential districts (ranging from low- to high-density single and multiple-family housing), commercial districts (from neighborhood and district commercial to central business districts, commercial corridors, and service commercial areas), industrial districts (light, service, and heavy industry, high-tech industrial parks, and warehousing), and social and institutional districts (educational and social facilities, civic facilities, and government facilities). Also included are leisure districts (open recreational fields, buffer zones, and tourist development areas), natural resource districts (date palm farming lands and nature reserves), and non-urban districts (no-development zone, future expansion area). The reference map is broken down by grid sections (A1–C4) for easy indication of a place as well as geographic coordinate data under UTM 38N WGS 1984 at a scale of 1:30,000. The project was prepared jointly with Al-Farbi Center for Development and Howgill Planning in a joint venture between local authorities and planning consultants to reflect the comprehensive urban sustainable development strategy for Kut city.

This figure also depicts the historical urban development of Kut over four different time slices between 1922 and 2025 that the researcher has prepared on the basis of the original final plan map from the above-cited source by making a digital overlay with Adobe Photoshop 2024. These periods indicate spatial growth and morphological transformation in the city during 20th as well as 21st centuries, starting from early core i.e.1930 to its projected urban extent till 2040. The municipal area is kept constant in all such phases of spatial development thereby increasing pressure on its activities and available space since it accommodates an increasing share of administrative, commercial, and social activities that continue to grow within the town itself. The UIR framework can be applied in Al-Kut, where zoning regulations consider it as pedestrian comfort strategies and heritage- sensitive urban renewal. Literature reviewed proves the concept of Urban Influence Radius: a quantifiable perimeter described by dimensions of height, street width, and baseline threshold through which the environmental influence of built form can be measured. Integrated as a metric into the urban policy for cities such as Al-Kut can have a method to improve the pedestrian thermal comfort and wind flow while keeping the environmental advantages in high-density contexts.

3. Concept and definition

The Urban Influence Radius is the perimeter around a project in the space within which its massing can measurably affect shading, ventilation, and thermal comfort as well as pedestrian performance and functional distribution. The size of the radius varies with land-use type, built density, coverage ratio and surrounding context [14], [15]. The formal definition is:

Eq. (1) $R = \max(2H, 1.5W, 60\text{ m})$

where H is the main building height and W is the adjacent street width. R is rounded to the nearest 5 m. Unless 2H or 1.5W is greater than 60 m, the baseline used is 60 m. This choice finds support in literature where aspect ratios and sky-view factors have been related to outdoor comfort and ventilation.

Al-Kut is the capital city of Wasit Province (approx.32.49°N, 45.82°E) also located on the Tigris River, by major road networks from Baghdad to southern cities that connect through here. It shares her borders with Baghdad Province to the north; Iran on the east; Maysan towards the south; and Dhi Qar in the west. Government buildings, traditional markets (suqs), and commercial corridors converge here making it a beehive of daily administrative, service, and economic activities. Over recent decades, improved connectivity and rising demand for housing and services have reshaped the center: buildings stand closer together, streets host a wider mix of uses, and public squares and pedestrian routes carry heavier daily flows than surrounding districts.

The historic core has largely kept its edges even as the city expanded across the river, tying new neighborhoods to the old heart and reinforcing its role as the primary destination for shopping, government errands, and social activity. The Tigris offers environmental benefits and riverfront amenity, though mounting urban pressures can limit how fully those advantages are realized [16], [17], [18], [19]. Within this framework, the designated city center (CC1) covers about 39 ha inside the 2010 urban fabric. The broader urbanized area measured 3,353 ha in 2010, with 1,174 ha planned for expansion to 2040 (total 4,566 ha). Policy CC1 guides infill and redevelopment to respect building lines and heights and requires façade/design approval, supporting a compact, walkable core with mixed residential–retail blocks up to four stories along key streets. On the river, Policy OS1 treats the Tigris waterfront as the city's principal landscape asset, calling for protection, enhancement, and

stitched linear parks and recreation along the corniche. Strategic growth prioritizes expansion eastward then arcing northwest, while Policy UF1 restricts building outside the urban boundary except in approved cases. Access is structured so all centers connect via main roads, with local streets providing comfortable, fine-grain links for residents and visitors [20].
Knowing how much urban influence gets in is a key look for checking how the city setup of Kut uses space and social factors. It shows a clear, stand-alone area giving different experiences and its closeness to the Tigris River splits up spaces and makes identity stronger. This makes it a suitable model, and its ratio between urban and landscape aligns with the development of Iraqi cities.

4. Methods

Methodologically, the study applies a quantitative workflow to the Dijla Hospital site in central Kut, evaluating performance both on site and within an Urban Influence Radius defined as R = max (2H, 1.5W, 60 m) and rounded to the nearest 5 m. A base model was built in Rhino and simulations were run in Grasshopper with Ladybug Tools after importing a Typical Meteorological Year EPW file. Key performance indicators include UTCI at the summer peak hour, winter solar hours on opposing façades for December to January, pedestrian-level wind change at 1.5 to 2.0 m relative to an unobstructed surrogate, the built-to-void ratio as a proxy for porosity, and walkability conflicts per 100 m. Analysis grids used 5 m on site and 5 to 10 m within the radius to balance runtime and spatial detail. Two massing scenarios were compared at nearly constant FAR ≈ 5.0, a high-coverage baseline and a lower-coverage alternative achieved by vertical redistribution without reducing program area. Decision thresholds for compliance follow Appendix A, and a sensitivity check varied R from 40 to 80 m and coverage from 50 to 80 percent to test robustness.

4.1. Case Study and area selection

The case site is Dijla Hospital, a high-occupancy institutional project located in the commercial core of Kut, Iraq. The surrounding fabric is dense and mixed use with medium street widths. The study boundary includes opposite façades and sidewalks that interact with the project at pedestrian level. Figure 2. Study area boundary in central Kut with the case site highlighted in red.

Figure 2. Study area: Dijla Central Hospital and adjacent riverfront neighborhoods on the Tigris, Al-Kut.

Hourly weather data were sourced from a Typical Meteorological Year file in EPW format and imported with Ladybug Import EPW. Summer analyses target the hottest design week based on UTCI and dry-bulb temperature. Winter analyses focus on December and January to capture minimum solar exposure.

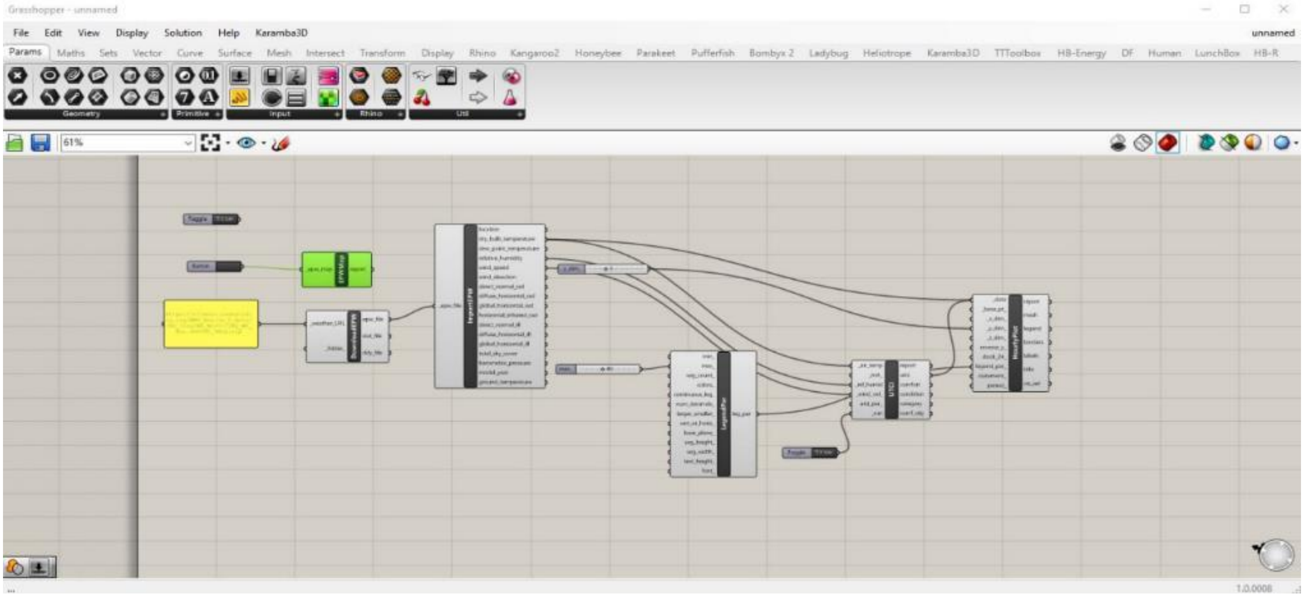

Figure 3. Import EPW and analysis period setup in Grasshopper.

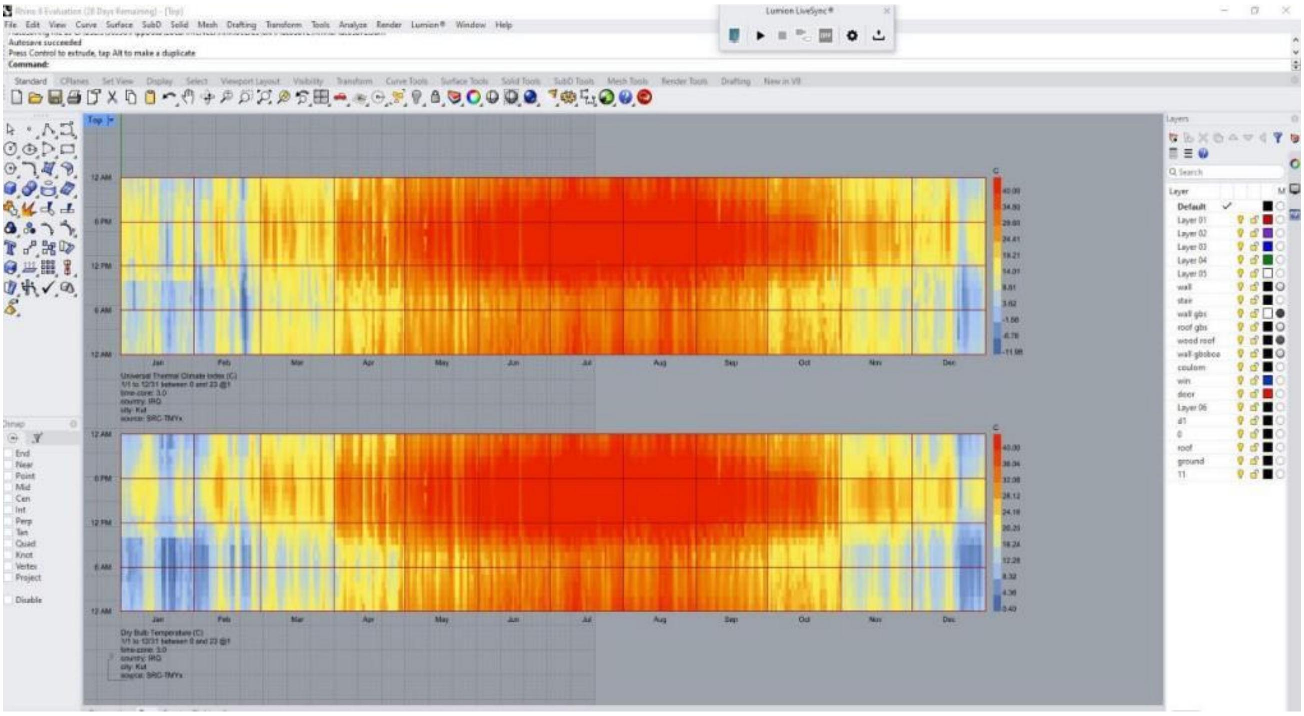

Figure 4. Annual climate charts for Kut.

4.2. Modeling and simulation

The base model was built in Rhino. Simulations were executed in Grasshopper with Ladybug Tools 1.8.x. A uniform analysis grid of 5 m was applied on site and a 5–10 m grid inside the Urban Influence Radius to balance runtime and detail. Direct Sun Hours was used for winter solar. The UTCI implementation in Ladybug Comfort evaluated thermal conditions in the summer peak hour. Pedestrian wind was assessed as percentage change at 1.5–2.0 m relative to an unobstructed surrogate during prevailing hours.

5. Results

Unless noted, R equals 60 m. KPI thresholds follow Appendix A. As shown in Figure 5, the alternative redistributes volume to increase porosity while keeping FAR ≈ 5.0. Figure 6 shows the climatic conditions and solar radiation limits adopted for the analysis at the study site; the left panel displays the dew point temperature-coded sun rose/path for Kut city to identify critical directions and seasons, while the right panel shows the direct sun hours map on the site geometry during the winter period (December-January).

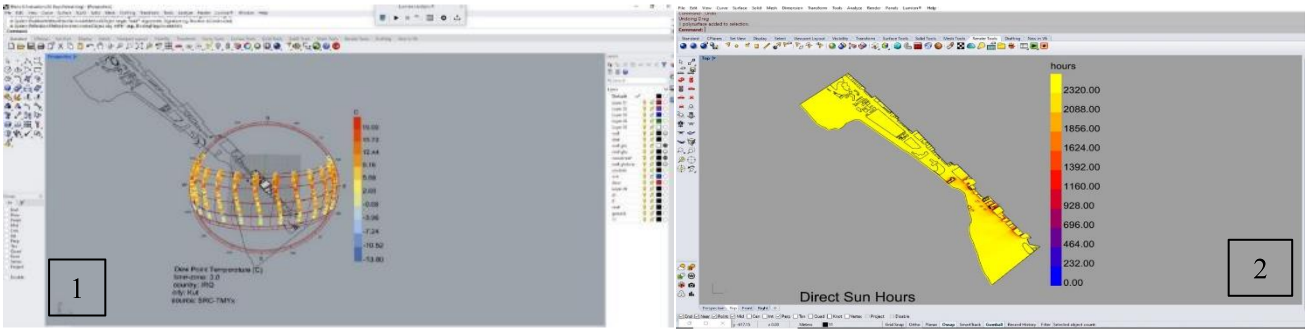

Figure 5. Climate rose (dew-point temperature) and Direct Sun Hours (Dec–Jan) for the study area, Al-Kut.

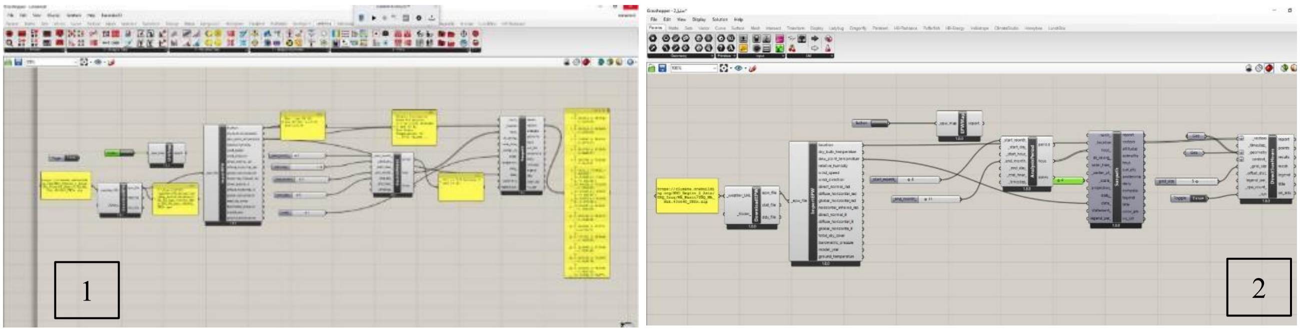

Figure 6. Grasshopper–Ladybug workflow for Al-Kut: EPW import, analysis-period setup, and climate-data pipeline with grid and legend outputs.

The figure introduces the Urban Influence Radius and the massing levers used to redistribute volume while keeping FAR ≈ 5.0. Panel (a) synthesizes the levers of connection, passage, and scale as operations that modify spacing, height offsets, and voids without reducing program area [5]. These operations affect sky-view factor, aspect ratios, and porosity, which in turn condition thermal stress and pedestrian-level ventilation.

The figure was developed by the researcher based on Ng's (2009) study on air ventilation assessment in high-density cities, and was further adapted to suit medium-density urban contexts [21].

Panel (b) formalizes the analytical perimeter and indicators. The Urban Influence Radius is defined as R= max (2H, 1.5W, 60m) where H is the principal height and W is the width of the adjacent street. Performance is assessed both on-site and within the UIR for five indicators: UTCI at the summer peak hour, winter solar access on opposing façades, pedestrian-level wind change, the built-to-void ratio as a proxy for porosity, and walkability conflicts per 100 m.

Panel (c) contrasts the two massing scenarios at equal program. The top-view diagrams compare the baseline high-coverage block with an alternative lower-coverage layout that increases porosity and permeability while preserving FAR. The figure anticipates the quantitative differences reported in Tables 1 and 2, where the alternative layout achieves lower UTCI, improved winter solar access, moderated corner winds with less stagnation, and fewer pedestrian conflicts.

5.1. Baseline scenario

Conditions are FAR about 5.0 and coverage about 80 percent. On-site average UTCI equals 34.7 °C with hotspots up to 39.8 °C. Within the Urban Influence Radius, the average is 33.6 °C and about 78 percent of samples exceed 29 °C which indicates heat stress that requires mitigation. Winter solar on opposite façades averages 2.3 h per day with a minimum of 1.4 h per day and 41 percent of façade segments fall below 2 h per day. Pedestrian wind shows a mean reduction of 18 percent in the radius relative to an unobstructed surrogate with corner accelerations of about plus 38 percent. Cells with a drop greater than 25 percent account for about 27 percent of the grid. Built to void ratio equals 2.8 to 1 with a local peak near 3.3 to 1. Walkability conflicts reach about 5.5 per 100 m along the main entrance and loading frontage.

5.2. Alternative scenario

Coverage is reduced to about 50 percent while FAR remains near 5.0. The UIR average UTCI drops by about 2.8 °C to 30.8 °C. The extent of hotspots shrinks by 35–40 percent and the share of samples above 29 °C falls from 78 percent to 42 percent. Average winter solar rises by 0.8 h per day to 3.1 h per day and the share below 2 h per day falls from 41 percent to 12 percent. Mean wind change improves to minus 6 percent which lies in the preferred band of minus 10 to plus 10 percent. Corner gusts are capped at about plus 26 percent and cells with drop greater than 25 percent fall from 27 percent to 8 percent. Built to void ratio improves to about 1.9 to 1 and conflicts drop to about 2.4 per 100 m.

5.3. Sensitivity analysis

Two dimensions were varied while keeping FAR near 5.0. Increasing R from 60 m to 80 m reveals additional winter shading with a reduction of about 0.6 h per day in average UIR solar access and about 11 additional façade segments below 2 h per day. Reducing coverage from 80 percent to 50 percent improves UIR wind by about 12 percentage points from minus 18 percent to minus 6 percent and raises winter solar by about 0.8 h per day. Benefits persist across R values of 40 m, 60 m, and 80 m.

5.4. Definitions and Metrics

The Floor Area Ratio (FAR) is the ratio of the total built floor area (all stories) to the plot area; it regulates the quantity of development but not how that volume is spatially distributed. By contrast, the Coverage Ratio measures only the building footprint divided by the plot area. Because pedestrian-level microclimate depends on distribution, via sky-view factor, aspect ratios, and ventilation paths, coverage and voids often exert stronger influence on outdoor comfort than FAR alone [22]. Targets used here follow common guidance: UTCI ≤ 26 °C as a comfort benchmark with 26 to 32 °C indicating moderate heat stress [23]; winter solar access ≥ 3 h/day on opposing façades (EN 17037-aligned practice) [24]; pedestrian wind criteria that constrain both stagnation and corner accelerations [25]; built-to-void as an operational proxy for porosity that supports ventilation [26] [27]; and walkability conflicts per 100 m as a frontage-friction measure sensitive to access management.

Tables 1 (baseline) and 2 (alternative) report key performance indicators within an Urban Influence Radius of R = 60 m while keeping the program area nearly constant (FAR ≈ 5.0). The baseline represents high coverage (~80%); the alternative reduces coverage to ~50% via vertical redistribution and added voids/setbacks. Indicators include UTCI at the summer peak hour, winter solar hours (Dec to Jan) on opposing façades, pedestrian-level wind change (mean and corner effects), the built-to-void ratio, and walkability conflicts. Targets and thresholds follow the sources cited above. Table 1 shows the baseline scenario key performance indicators (KPIs) within the UIR model, including measured values, target thresholds, decision limits, and overall ratings.

Table 1. Baseline Scenario KPIs and Ratings.

Indicator	Metric and Unit	UIR, R ≤ 60 m	Target	Decision Threshold	Rating
UTCI	°C at summer peak hour	33.6	≤ 26	> 29 requires shading and porosity	Very Poor
Winter solar	h per day Dec–Jan	2.3 avg, 1.4 min	≥ 3	< 2 requires height and spacing changes	Poor
Wind change	percent at 1.5–2.0 m	–18 avg, +38 corners	–10 to +10	drop > 25 or increase > 35	Moderate to Poor
Built to void	solid to void	2.8:1 peak, 3.3:1	≤ 2:1	> 3:1 requires setback or lower coverage	Poor
Walkability	conflicts per 100 m	5.5	≤ 2	≥ 6 requires rerouted access	Poor

Table 2 shows the key performance indicators for the alternative scenario within the (KPIs) within the UIR model, highlighting measured values, target thresholds, decision limits, and the corresponding ratings.

Table 2. Alternative Scenario KPIs and Sating.

Indicator	Metric and Unit	UIR, R ≤ 60 m	Target	Decision Threshold	Rating
UTCI	°C at summer peak hour	30.8	≤ 26	> 29 requires shading and porosity	Moderate
Winter solar	h per day Dec–Jan	3.1 avg, 2.2 min	≥ 3	< 2 requires height and spacing changes	Good
Wind change	percent at 1.5–2.0 m	−6 avg, corners ≤ +26	−10 to +10	drop > 25 or increase > 35	Good
Built to void	solid to void	1.9:1	≤ 2:1	> 3:1 requires setback or lower coverage	Good
Walkability	conflicts per 100 m	2.4	≤ 2	≥ 6 requires rerouted access	Good

UTCI within the UIR falls from 33.6 °C (baseline) to 30.8 °C (alternative) a −2.8 °C improvement. Both are above the ≤ 26 z°C target, however, the shift is toward lower bound of moderate heat stress and quite consistent with an apparent reduced coverage and increased porosity that would mitigate radiant and convective loads at pedestrian level [26], [23]. Winter solar access increases from 2.3h/day(min1.4h) to 3.1h/day(min2.2h), moving closer toward achieving the ≥ 3h/day objective with more spacing and repassing [24]. Pedestrian wind conditions improve because the mean wind change moves from −18% (stagnation) to −6% in the preferred −10%to+10%bandand corner gusts drop from +38%to≤+26%. Though the metric above is of a relative change and not an exceedance-probability class, its direction coincides with Lawson-type criteria that are meant towards the avoidance of both severe corner accelerations and excessive stagnation around tall massing. The built-to-void ratio moves from 2.8:1 (peak 3.3:1) to ≈ 1.9:1 approaching the ≤ 2:1 target reflecting greater porosity that renews pedestrian-level airflow. Finally, walkability conflicts fall from 5.5 to 2.4 per 100 m almost meeting the ≤ 2 target aligning with access-management guidance that consolidates driveways reducing frontage conflict points thus improving pedestrian safety and level of service.

Compared to the baseline, the alternative goes in the right direction: less thermal stress, better winter sun access, improved pedestrian wind conditions, a more open built to void ratio, and reduced frontage conflicts. It makes a good illustration in that comfort is above target and corner accelerations remain an issue while walkability has not attained its intended threshold. Further improvement should focus on modest reductions in coverage with corner setbacks and added porosity, targeted shading on sun exposed facades, and tighter access management to reduce conflict points while preserving the winter solar gains.

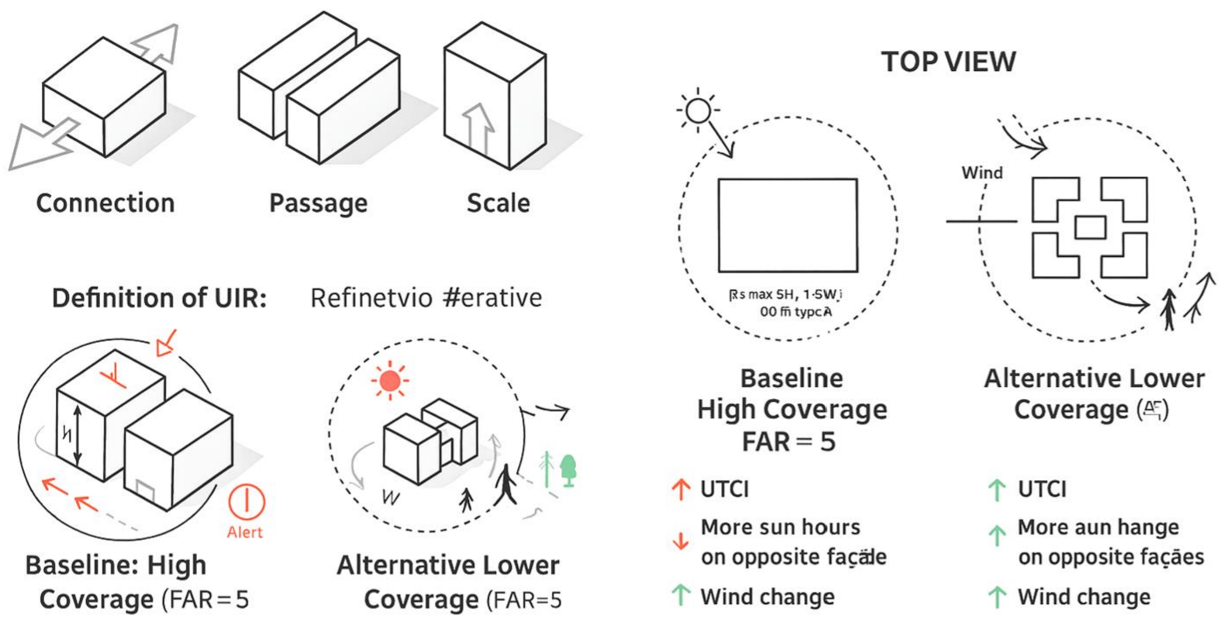

Figure 7. Conceptual Representation of Urban Influence Radius Components (URI) and Coverage Scenarios

This study is original in the sense that it describes the Urban Influence Radius (UIR) as a tangible spatial envelope that helps to connect on-and off-site effects and takes the assessment beyond the boundaries of a plot. Building height and occupancy relate functionally and environmentally to extend their influence when compared with conventional regulations where building height and setback only relate to control of shading, which has been characterized in the proposed framework over increased user density, disruption of air flow, and pedestrian activity. As illustrated in Figure 7, the UIR captures not only geometric parameters such as scale, connection, and passage, but also their implications for comfort and circulation within a continuous urban field. This framework thus introduces a scalable and replicable metric for evaluating environmental–spatial interdependence in densifying medium-sized cities.

6. Discussion

Projects with identical FAR can deliver different outcomes once off-site effects are measured. Under high coverage, the Urban Influence Radius exhibits elevated UTCI, winter under-illumination on opposing façades, and both stagnation and corner accelerations in the wind field. Lower coverage with vertical redistribution improves thermal comfort, winter solar access, and wind renewal while preserving program area. These findings agree with literature on the roles of sky-view factor, aspect ratio, and porosity in outdoor comfort and ventilation [26], [27], and with widely used pedestrian-wind criteria that balance threshold speeds and exceedance probabilities [25]. Because FAR controls quantity but not distribution, coverage emerges as a dominant lever for environmental performance in dense mixed-use cores.

7. Conclusions

This study formalizes the Urban Influence Radius as a measurable perimeter for off-site effects and demonstrates a replicable, threshold-based workflow for parallel on-site and UIR reporting. With FAR held near 5.0, lowering site coverage by redistributing mass improved all off-site KPIs inside the UIR: UTCI decreased, winter solar access met the 3 h objective, pedestrian wind moved into the preferred −10 to +10 band with lower corner gusts, built-to-void approached ≤ 2:1, and walkability conflicts declined toward ≤ 2 per 100 m. The UTCI comfort target (≤ 26 °C) was not fully met, but heat stress shifted downward in a meaningful way.

Future research may integrate virtual reality (VR) platforms and immersive simulation tools to visualize and interactively assess spatial comfort and environmental performance within the Urban Influence Radius. Such integration can enhance stakeholder understanding and strengthen design-based decision support in medium-sized cities.

Overall, volume distribution matters as much as volume quantity. Because FAR regulates total floor area but not its allocation, coverage and effective porosity are the principal levers for environmental performance in dense mixed-use cores. Approvals should incorporate UIR screening with explicit thresholds and require threshold-driven iteration so that off-site effects are evaluated alongside on-site compliance.

8. Appendix A. KPI bands and rating scale

Standard-based bands: UTCI [23] and winter solar access informed by EN 17037 and BRE guidance [24].

Proposed for this study: wind change expressed as a relative percent within the UIR with cross-reference to Lawson-type comfort checks [25]; built-to-void as a porosity proxy informed by the ventilation literature [26], [27]; and walkability conflicts per 100 m informed by access-management guidance. Bands are intended for screening and can be calibrated to local climate and street typologies.

A.1 Standard-based bands

- UTCI, in °C at summer peak hour
- Excellent: ≤ 26
- Good: 26.1 to 28
- Moderate: 28.1 to 29.5
- Poor: 29.6 to 31
- Very Poor: > 31

Winter solar access, hours per day (Dec–Jan) on opposing façades

- Excellent: ≥ 3.0
- Good: 2.5 to 2.9
- Moderate: 2.0 to 2.49

- Poor: 1.5 to 1.99
- Very Poor: < 1.5

A.2 Proposed bands for this study

Wind change, percent at 1.5–2.0 m (relative change within the UIR)

- Excellent: within −10% to +10%
- Good: absolute deviation of 10 to 15 percentage points
- Moderate: absolute deviation of 15 to 25 percentage points
- Poor: ≤ −25% or ≥ +35%
- Very Poor: ≤ −35% or ≥ +50%

Built-to-void, solid-to-void ratio

- Excellent: ≤ 2:1
- Good: 2.01:1 to 2.5:1
- Moderate: 2.51:1 to 3:1
- Poor: 3.01:1 to 3.5:1
- Very Poor: > 3.5:1

Walkability conflicts per 100 m

- Excellent: ≤ 2
- Good: 3
- Moderate: 4
- Poor: 5
- Very Poor: ≥ 6

Thresholds may be adapted to local climate and street geometry. For instance, UTCI upper bounds can be adjusted in extremely hot regions, while wind bands may be tightened near sensitive frontages (e.g., hospital entrances or schools).

9. Author Contributions

Haider Majid Hasan led the conceptualization and methodology selection, compiled recent sources, wrote the final results, and provided full supervision. Husam Sachet Saneh, and Ayam Sh. Altameemi conducted the environmental analysis using Rhino with Grasshopper and Ladybug Tools. Noor Dheyaa Joodi prepared the existing case study base maps in GIS and documented the case study. All authors discussed the work collectively, contributed to the interpretation, and agreed on the overall findings and recommendations.

10. Acknowledgment

Thanks to Kut Municipality and Wasit Urban Planning Directorate who provided information on the site and reports about development for this area of study.

11. References

[1] F. Ali-Toudert and H. Mayer, “Numerical study on the effects of aspect ratio and orientation of an urban street canyon on outdoor thermal comfort in hot and dry climate,” *Build Environ*, vol. 41, no. 2, pp. 94–108, 2006, doi: 10.1016/j.buildenv.2005.01.013.

[2] O. Palusci, P. Monti, C. Cecere, H. Montazeri, and B. Blocken, “Impact of morphological parameters on urban ventilation in compact cities: The case of the Tuscolano-Don Bosco district in Rome,” *Science of the Total Environment*, vol. 807, Feb. 2022, doi: 10.1016/j.scitotenv.2021.150490.

[3] Y. Wang, M. Qi, and Y. Lu, “A parametric study of urban ventilation corridors for improving air quality in compact cities,” *J Clean Prod*, vol. 500, p. 145219, 2025, doi: https://doi.org/10.1016/j.jclepro.2025.145219.

[4] Q. Guo, Y. Lin, and X. Zhang, “Identification and cooling effect analysis of urban ventilation corridors in coastal hilly cities: A case study of Shenzhen,” *Urban Clim*, vol. 61, p. 102393, 2025, doi: https://doi.org/10.1016/j.uclim.2025.102393.

[5] C. Zhao, “Intelligent extraction of urban ventilation corridors based on region growth algorithm with restricted direction,” *Sci Rep*, vol. 15, no. 1, Dec. 2025, doi: 10.1038/s41598-025-01804-7.

[6] H. S. O. Aldelphi, “Urban Visual Quality Of Traditional Kut City Center,” *no*, vol. 7, pp. 57–64, 2019.

[7] I. A. Jasim, H. M. Hasan, S. L. Farhan, and K. H. Bahat, “Evaluating the urban structure of Al-Kut city according to sustainability,” in *IOP Conference Series: Earth and Environmental Science*, IOP Publishing Ltd, Jul. 2021. doi: 10.1088/1755-1315/779/1/012021.

[8] I. A. Jasim, S. L. Farhan, and A. T. Attalla, “Sustainable neighborhood comparative analysis of Al Kut neighborhoods,” *Journal of University of Babylon for Engineering Sciences*, vol. 26, no. 9, pp. 302–317, 2018.

[9] H. S. O. Aldelphi, “المثنى للهندسة والتكنولوجيا . Urban Visual Quality Of Traditional Kut City Center,” vol مجلة .no. 7, pp. 57–64, 2019, doi: 10.18081/mjet/2019-7/57-64, 57

[10] Z. Mohammed, A. Ziboon, A. Kamal, and M. Alfaraj, “Urban air quality evaluation over Kut city using field survey and Geomatic techniques,” in *MATEC Web of Conferences*, EDP Sciences, Mar. 2018. doi: 10.1051/matecconf/201816205023.

[11] S. Alhussen and Husam Sachit Senah, “Urban Landscape Resilience: Reconnecting the River with Al-Kut’s Traditional City Centre,” *Wasit Journal of Engineering Sciences*, vol. 12, no. 4, pp. 191–202, Dec. 2024, doi: 10.31185/ejuow.Vol12.Iss4.590.

[12] S. Alhussen and H. S. Senah, “Urban Landscape Resilience: Reconnecting the River with Al-Kut’s Traditional City Centre,” *Wasit Journal of Engineering Sciences*, vol. 12, no. 4, pp. 191–202, Dec. 2024, doi: 10.31185/ejuow.Vol12.Iss4.590.

[13] R. J. Al-Shammari and A. Na’im Mohsin, “Visual Sustainability in Urban Renewal Projects Traditional kut City Center as a Case Study,” *Wasit Journal of Engineering Sciences*, vol. 12, no. 1, Jan. 2024, doi: 10.31185/ejuow.vol12.iss1.516.

[14] J. Yin, Q. Zhan, M. Tayyab, and A. Zahra, “The ventilation efficiency of urban built intensity and ventilation path identification: A case study of Wuhan,” *Int J Environ Res Public Health*, vol. 18, no. 21, Nov. 2021, doi: 10.3390/ijerph182111684.

[15] L. Zeng *et al.*, “Influence of Various Urban Morphological Parameters on Urban Canopy Ventilation: A Parametric Numerical Study,” *Atmosphere (Basel)*, vol. 15, no. 3, Mar. 2024, doi: 10.3390/atmos15030352.

[16] S. L. Farhan, I. A. J. Hashim, and A. A. Naji, “The sustainable house: Comparative analysis of houses in Al Kut Neighborhoods-Iraq,” in *2019 12th International Conference on Developments in eSystems Engineering (DeSE)*, IEEE, 2019, pp. 1031–1036.

[17] R. Al-Anbari, A. Alnakeeb, and S. Lafta Farhan, “Appraisal Criteria-Space in some Residential Urban Areas for Al-Kut City,” 2014.

[18] I. Abbass Jasim, S. Lafta Farhan, and S. Kareem AL-MAMOORI, “Smart Government: Analysis of Shift Methods in Municipal Services Delivery: The Study Area: Al-Kut-Iraq.”

[19] S. F. Balket and N. M. Asmael, “Selecting the best route location for bus rapid transit using geographic information system (gis): Kut city is a case study,” in *Journal of Physics: Conference Series*, IOP Publishing Ltd, Jun. 2021. doi: 10.1088/1742-6596/1895/1/012029.

[20] *Ministry of Municipalities and Public Works, Directorate of Urban Planning, Wasit Governorate, Master Plan of Al-Kut City: Final Basic Plan, Phase Six Report, Part I: Policies and Proposals, Al-Farabi Center for Development and Haubin Planning, Sept. 2013*

[21] E. Ng, “Policies and technical guidelines for urban planning of high-density cities - air ventilation assessment (AVA) of Hong Kong,” *Build Environ*, vol. 44, no. 7, pp. 1478–1488, Jul. 2009, doi: 10.1016/j.buildenv.2008.06.013.

[22] S. K. G. H. C. T. & A. Longfield. Paul Littlefair, *Site layout planning for daylight and sunlight: a guide to good practice (BR 209 2022 edition - Download) [PDF]*. BRE Electronic Publications, 2022.

[23] K. Błazejczyk *et al.*, “An introduction to the Universal thermal climate index (UTCI),” *Geogr Pol*, vol. 86, no. 1, pp. 5–10, 2013, doi: 10.7163/GPol.2013.1.

[24] A. Tabadkani, A. Roetzel, H. X. Li, and A. Tsangrassoulis, “Daylight in buildings and visual comfort evaluation: The advantages and limitations,” Dec. 01, 2021, *Solarlits*. doi: 10.15627/jd.2021.16.

[25] C. of London Corporation, “City of London Wind Microclimate Guidelines.”

[26] C. Yuan and E. Ng, “Building porosity for better urban ventilation in high-density cities - A computational parametric study,” *Build Environ*, vol. 50, pp. 176–189, Apr. 2012, doi: 10.1016/j.buildenv.2011.10.023.

[27] Y. Du, C. M. Mak, and B. Tang, “Effects of building height and porosity on pedestrian level wind comfort in a high-density urban built environment,” *Build Simul*, vol. 11, no. 6, pp. 1215–1228, 2018, doi: 10.1007/s12273-018-0451-y.